arXiv:1606.07990v1 [physics.atom-ph] 26 Jun 2016

Tuning Casimir-Polder interactions in atom-metamaterial hybrid devices

Eng Aik Chan,[1] Syed Abdullah Aljunid,[1] Giorgio Adamo,[1] Athanasios Laliotis,[2] Martial Ducloy,[1,2,3,*] and David Wilkowski[1,4,5,3,†]

[1] *Centre for Disruptive Photonic Technologies, TPI, Nanyang Technological University, 637371 Singapore*
[2] *Laboratoire de Physique des Lasers, UMR 7538 du CNRS, Université Paris13-Sorbonne-Paris-Cité F-93430 Villetaneuse, France*
[3] *School of Physical and Mathematical Sciences, Nanyang Technological University, 637371, Singapore*
[4] *Centre for Quantum Technologies, National University of Singapore, 117543 Singapore*
[5] *MajuLab, CNRS-Université de Nice-NUS-NTU International Joint Research Unit UMI 3654, Singapore*

(Dated: June 28, 2016)

We report on the coupling of a surface plasmonic mode with a thermal vapor of cesium atoms. The plasmonic resonance is created using a nano-structured metallic surface. By changing the geometrical properties of the metamaterial, we tune the plasmonic resonance wavelength with respect to the D2 line of cesium. When the two resonances are close, we observe a strong modification of the Casimir-Polder interaction accompanied by a change of the atomic lifetime. A proper tuning leads to an almost suppression of the frequency shift of the cesium transition. This result paves the way for precision atomic spectroscopy in the vicinity of a material surface.

PACS numbers: 34.50.Dy, 78.67.Pt, 32.90.+a, 78.20.-e

The Casimir-Polder or van der Waals interaction between an atom or a molecule, and a flat material surface has been, for many years, considered as a pure academic problem of quantum hybrid systems [1–6]. With the advances of experimental techniques in the 70's, deflection of long-lived internal states in beams on material surfaces have been studied [7]. Later, the development of new spectroscopic approaches, such as Selective Reflection [8, 9], and ultra-thin vapor cells [10], extends atom-surface investigations to short-lived radiative states. Casimir-Polder interactions have also been measured by trapping cold atoms in the vicinity of dielectric surfaces [11, 12]. Recently, the atoms/surface interaction problem gained new interest in the effort to merge ultracold gases and nanotechnologies with prospects in sensing, quantum information and atoms trapping [13–15]. In this respect, the Casimir-Polder interaction may appear as a limiting factor since it induces position-dependent atomic frequency shifts and attractive forces.

One approach to modify the Casimir-Polder interaction relies on the resonant coupling between excited atoms and surface resonances. Here, the resonantly-enhanced interaction potential can be turned into a repulsive potential, as it has been demonstrated on excited Cesium atoms interacting with surface polaritons on dispersive sapphire surfaces [16]. The various approaches used to tune the polariton frequency, such as material birefringence [17] and surface temperature [18], share the restriction that the dielectric surface polaritons reside in the far infrared spectral region, implying that only highly excited atoms exhibit near-resonant coupling with the dielectric material.

In this letter, we take advantage of the broad spectral tunability of plasmonic resonances to extend atom-surface resonant coupling to low-lying atomic states. More precisely, we use thin metallic planar metamaterials to combine the advantages of wavelength-tunable localized surface plasmons together with enhanced light transmission at the plasmon resonance. The Casimir-Polder interaction of Cesium thermal vapor with silver metasurfaces is investigated here. We observe that the Casimir-Polder shift of the $6S_{1/2} \rightarrow 6P_{3/2}$ Cesium D2 transition exhibits a resonant behaviour for surface dispersion forces, as well as a near-field dissipative coupling [19]. For an adequately chosen metasurface, the frequency shift on the Cesium transition, induced by the Casimir-Polder interaction, can be almost suppressed.

The system under investigation is depicted in Fig. 1a. A cesium vapor at $T = 80\,^{\circ}\mathrm{C}$ is introduced into a vacuum chamber. The density of the atoms is around $N = 10^{17}\,\mathrm{m}^{-3}$ whereas the thermal velocity is $\bar{v} = 150\,\mathrm{ms}^{-1}$. On one of the dielectric viewport of the vacuum chamber, ten different metamaterials are engraved on an $l = 50\,\mathrm{nm}$ thick silver layer (see Fig. 1b). An 8 nm film of SiO_2 is deposited on top to avoid oxidation of the silver layer. Each metamaterial consists of a $200 \times 200\,\mu\mathrm{m}^2$ square area of a $\sim$ 400 nm periodic array of nano-slits. The metamaterials are characterized by the centre of their main plasmonic resonances, covering a wavelength range from 670 nm to 980 nm [20]. Each plasmonic resonance has a typical width of 60 nm (see an example in Fig. 1c).

The atoms/metamaterial hybrid system is excited and probed on the $6S_{1/2} \rightarrow 6P_{3/2}$ cesium D2 transition at 852 nm, using a Selective Reflection optical setup at normal incidence [8]. The radiation is produced by an external cavity diode laser (ECDL). Part of the light is sent to a saturated absorption spectroscopy setup as a frequency reference. The main beam is passing through an

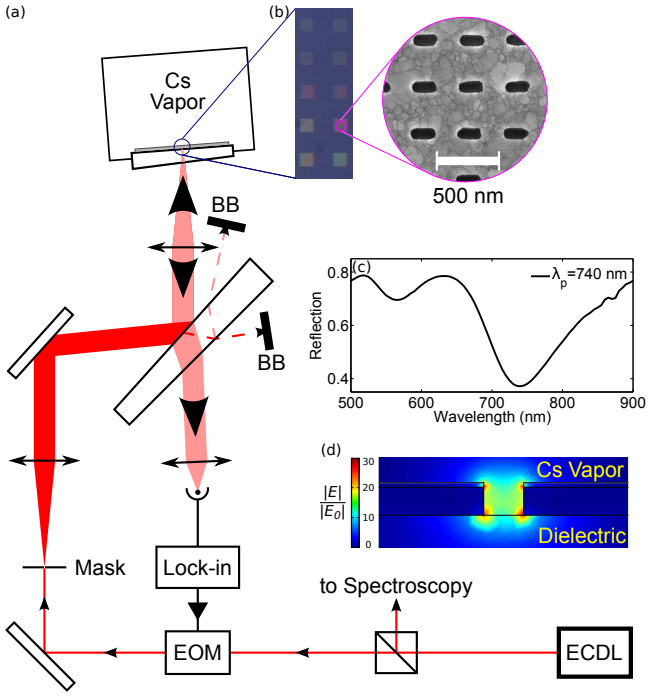

Figure 1. (a) Experimental set-up. (b) Real color back-illuminated images of the ten metamaterials. The zoom corresponds to an SEM image. (c) A typical reflectance curve of a metamaterial showing a main plasmonic resonance at $\lambda_p = 740\,\mathrm{nm}$. (d) Cut along one nanoslit. The false colors represent the electric field magnitude obtained by FEM simulation.

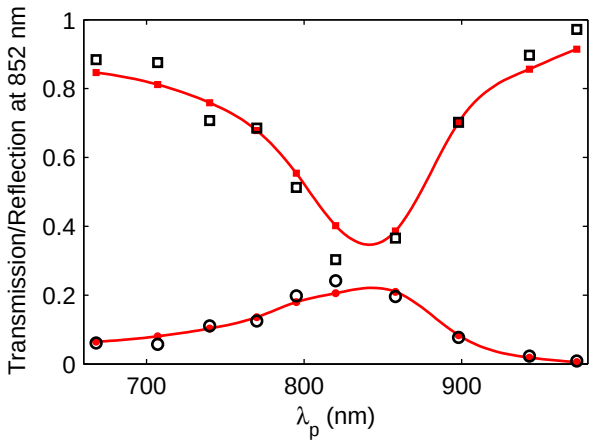

Figure 2. Experimental reflection (open squares) and transmission (open circles) of the ten metamaterials for $\lambda = 852\,\mathrm{nm}$. The x-axis corresponds to λ_p, the position of the plasmonic resonance of each metamaterial. The solid red squares (circles) corresponds to the reflection (transmission) obtained by FEM numerical simulation. The lines, connecting FEM results, are guides for the eye.

Electro-Optic Modulator (EOM) to modulate its phase at $\Omega_m = 9\,\mathrm{MHz}$ with a modulation index of $\beta = 0.19$. Further, the beam is shaped by a square mask to optimize the overlapping between the beam and the metamaterial. The intensity of the laser is maintained below saturation, typically $I = 1\,\mathrm{mWcm}^{-2}$, at the level of the atomic vapor. The reflected light beam is collected on a fast and sensitive amplified photodetector. The signal at 9 MHz is demodulated using a lock-in amplifier.

First, we analyze the reflectance and transmittance intensities of the metamaterials. To do so, we detuned the laser away from the cesium resonance such that it is not coupled anymore to the atomic vapor whereas the coupling to the plasmon remains unchanged. The results are summarized in Fig. 2. Here, each pair of reflectance/transmittance data corresponds to a given metamaterial, which is characterized by its centre resonance frequency, λ_p, reported on the x-axis of the graph. The resulting curves show a smooth resonance-like behavior, indicating that all the metamaterials have a similar reflectance and transmittance spectrum (see also [20]). For a more quantitative analysis, we perform a Finite Element Methods (FEM) simulation of the metamaterials. We extract the expected far-field reflectance and transmittance intensities of the metamaterials. The FEM results are in good agreement with the experimental data. However, we perform a global adjustment of the contrast of the reflectance and transmittance of the FEM results by a factor of 0.7 and 0.5 respectively. This adjustment accounts for frequency independent optical losses, not encountered in the FEM simulation. Contributions may come from photon scattering at the metamaterials, imperfect size matching of the beam to the metamaterial or possible long range inhomogeneity of the metamaterial geometry.

We now tune the laser onto the $F = 4 \rightarrow F = 5$ hyperfine transition over a frequency range of 100 MHz $\simeq 20\Gamma/(2\pi)$, where $\Gamma = 2\pi \times 5.2\,\mathrm{MHz}$, is the bare frequency width of the atomic transition. The demodulated signals at 9 MHz of the beam reflectance correspond to the red points on Fig. 3. We observe a strong modification of the spectrum due to the presence of the metamaterials with respect to a plain dielectric window (see blue points on Fig. 3)

To further analyze the experimental data, we assume that the metamaterial can be modeled by a spatially homogeneous bulk material having the same thickness and the same far-field properties at normal incidence. Then following references [21], we deduce, n, the complex index of refraction of the effective bulk material. If this mean-field approximation is known to give excellent results in the far-field [21], it may be questioned here, since the reflectance signal of the atomic vapor emerges from the response of the atoms in the vicinity of the metamaterial [8]. We tried to test the validity of this approach by solving the optical-Bloch equation for two-level atoms flying above the metamaterial surface at thermal velocity. We find that the atomic response, across the variations of

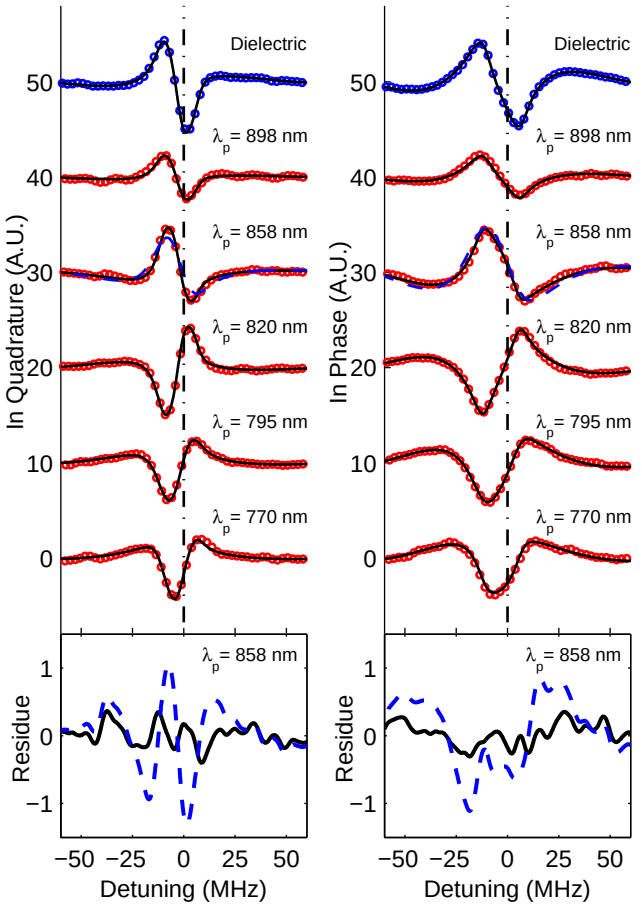

Figure 3. In phase and in quadrature selective reflection spectra of the plain windows (blue dots at top curves) and of five metamaterials (red dots). The black solid curves are the fits using Eqns. 1–5. The dashed blue line is a fit setting $\mathrm{Im}[C_3] = 0$. The residues correspond to the metamaterial with a resonance at $\lambda_p = 858\,\mathrm{nm}$.

the electric field over the metamaterial unit cell (see example in Fig. 1d), is well smoothed because of the finite response time of the atomic coherence. Thus, only the averaged electric field can be considered meaningful, implying that the mean-field approximation is reasonable.

For Selective Reflection (SR), the vapor is characterized by an effective electric susceptibility Its frequency derivative is given, in the Doppler limit ($k\bar{v} \gg \Gamma$), by [22]

$$\frac{\mathrm{d}\chi(\omega)}{\mathrm{d}\omega} = \imath\frac{2Nk\mu^2}{\sqrt{\pi}\bar{v}\epsilon_0\hbar} \times \int_0^{+\infty}\mathrm{d}z\int_0^{+\infty}\mathrm{d}z'\frac{(z-z')\mathrm{e}^{\imath k(z+z')}}{\mathcal{L}_0(\omega,z)-\mathcal{L}_0(\omega,z')}. \quad (1)$$

$\mathcal{L}_0(\omega,z)/z = \Gamma/2 - \imath(\omega-\omega_0+C_3\hbar^{-1}z^{-3}/2)$ is the Lorentzian lineshape of the bare atomic resonance, corrected by the $1/z^3$ Casimir-Polder frequency shift (in the non-retarded regime). C_3 is the van der Waals coefficient, ω_0 is the bare atomic resonance, k is the wavenumber of the beam and μ is the two-level atomic dipole moment. The metamaterial/vapor interface is located at $z = 0$. We note that the phase factor, $\exp(\imath k(z+z'))$ rapidly averages the effective susceptibility to zero for $z, z' \gtrsim k^{-1}$. As an important consequence, only the atoms located in a layer of thickness k^{-1} contribute to the SR signal. Moreover, as it can be seen in Eqn. (1), the signal is Doppler-free. Indeed atoms with velocity components normal to the metamaterial surface, experience strong coherence relaxation due to collision with the surface. They do not contribute to the SR signal. We note as well that, since $\chi \ll 1$, the index of refraction of the atomic vapor reads as $n_a \simeq 1+\chi/2$. Under this approximation, the complex reflection coefficient of the electric field for the dielectric/metamaterial/vapor system can be linearized as,

$$r = r_0 + \rho\chi, \quad (2)$$

where r_0 and ρ depend only on the indices of refraction of the metamaterial n and of the dielectric substrate n_d. In the Doppler limit, $\chi(\omega)$ is obtained by a frequency integration of Eqn. (1). In the weak modulation limit, i.e. $\beta \ll 1$, we find that the demodulated signal has the following expression for the in-phase signal,

$$V_p(\omega) = V_0\,\mathrm{Re}\{r_0^*\rho[\chi(\omega+\omega_m)-\chi(\omega-\omega_m)]\}, \quad (3)$$

and for the in-quadrature signal,

$$V_q(\omega) = V_0\,\mathrm{Im}\{r_0^*\rho[\chi(\omega+\omega_m)+\chi(\omega-\omega_m)-2\chi(\omega)]\}. \quad (4)$$

V_0 is a factor of proportionality. Within the mean-field approximation, the complex factor $r_0^*\rho$ can be evaluated analytically as in [23],

$$r_0^*\rho = \frac{8n_d\mathrm{e}^{2\imath nl\omega/c}}{(1+n)^2(n^2-n_d^2)+2(1-n^2)(n_d^2+n^2)\mathrm{e}^{2\imath nl\omega/c}+(1-n)^2(n^2-n_d^2)\mathrm{e}^{\imath nl\omega/c}}, \quad (5)$$

where l is the metamaterial thickness. By mixing the real and imaginary part of the susceptibility, it gives the main contribution of the modification of the atomic resonance lineshape induced by the plasmonic resonance observed in Fig. 3. Also, the complex origin of the factor $r_0^*\rho$ leads to Fano-like resonance of the atoms/metamaterial hybrid system as discussed in [20].

Using Eqns. (1)–(5), we perform a fit of the SR signals

for the different metamaterials including the bare dielectric substrate. The fitting parameters are the atomic resonance linewidth Γ, the complex value of C_3 and a common V_0 value. The index of refraction of the metamaterial n, thus the factor $r_0^*\rho$, is extracted from the FEM simulation. The results of the fitting procedure correspond to the black curves in Fig. 3. We observed an excellent agreement with the experimental data. The atomic resonance width is found to be 10(3) MHz, i.e. slightly larger than the bare linewidth of 5.2 MHz. This increasing of the linewidth, encountered as well on the dielectric interface, has been also reported on similar studies [9]. It can be due to residual Doppler or collisional broadening.

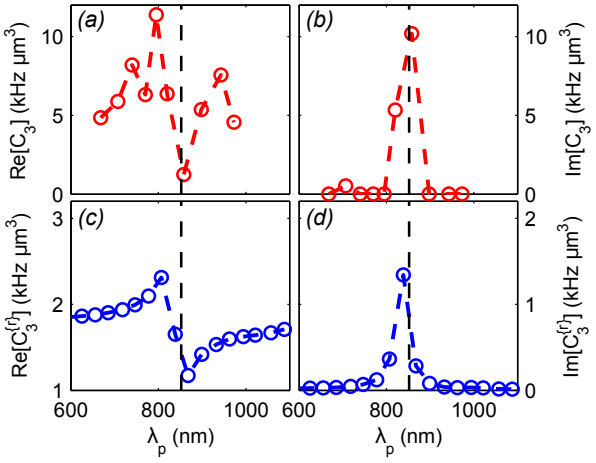

Figure 4. Real part (a) and imaginary part (b) of the C_3 coefficients extracted from the fits. (c) and (d) are the real and imaginary parts of the $C_3^{\{r\}}$ coefficients deduced from the model (see text for more details). We take $\mu_r = 2.6 \times 10^{-29}$ Cm. The vertical dashed lines indicate the position of the atomic resonance.

Importantly, an imaginary part for the C_3 has to be considered. To illustrate this point, we perform another fit, setting $\mathrm{Im}[C_3] = 0$. Under this constraint, we observe that the convergence of the fitting procedure is not satisfactory (see residue comparison in Fig. 3 for $\lambda_p = 858$ nm). The complex C_3 van der Waals coefficients obtained from the fits are shown in Fig. 4a-b. We observe a resonant behavior with a nearly vanishing value on the red side of the resonance. The resonance width is in agreement with the plasmonic linewidth of 60 nm, confirming the plasmonic origin of the modification of the C_3 values.

An analysis of the resonance behavior of the Casimir-Polder interaction, in the non-retarded regime, can be done using a simple model where the C_3 coefficient is decomposed into two components [24, 25],

$$C_3 = C_3^{\{\mathrm{nr}\}} + C_3^{\{\mathrm{r}\}}. \tag{6}$$

Here $C_3^{\{\mathrm{nr}\}}$ takes into account the dispersion contribution of virtual exchange of non-resonant vacuum photons, whereas $C_3^{\{\mathrm{r}\}}$ gives the contribution due to resonant photon exchange between an excited atom and the metamaterial. The $C_3^{\{\mathrm{nr}\}}$ is practically independent of the plasmonic resonance position and is mostly governed by the metallic response over the entire frequency spectrum [24, 25]. As such, its calculation is not necessary here. The influence of the plasmonic resonance is contained in the $C_3^{\{\mathrm{r}\}}$ since it concerns only the resonant photons emitted on the $6\mathrm{P}_{3/2} \rightarrow 6\mathrm{S}_{1/2}$ cesium D2 transition at 852 nm. Following reference [25], we predict,

$$C_3^{\{\mathrm{r}\}} = \frac{\mu_r^2}{24\pi\epsilon_0}\frac{\epsilon - 1}{\epsilon + 1}, \tag{7}$$

where ϵ is the complex dielectric constant of the metamaterial extracted from the FEM simulation and μ_r the reduced dipole moment matrix element of the $6\mathrm{P}_{3/2} \rightarrow 6\mathrm{S}_{1/2}$ coupling. $\mathrm{Re}[C_3^{\{\mathrm{r}\}}]$ yields the atomic frequency shift and $\mathrm{Im}[C_3^{\{\mathrm{r}\}}]$ the metamaterial-induced dissipative coupling. The results of this non-retarded model are shown in Fig. 4c-d. The theoretical predictions exhibit a resonant behavior similar to the experimental findings. However, the amplitude of the resonance is smaller than the experimentally measured one. Reductions of C_3 amplitude were also reported in other studies [9]. An accurate comparison will need a more refined theoretical model taking into account the non-negligible retardation effects, the finite thickness of the metamaterial, the strong anisotropy of its effective dielectric constant and deviations from the mean-field approximation. A proper treatment of those aspects is beyond the scope of this letter and will be addressed in a future publication [26].

To conclude, we use planar metamaterials to control the Casimir-Polder frequency shift of the D2 line of cesium atoms. When the plasmonic resonance almost coincides with the atomic resonance, the Casimir-Polder frequency shift nearly vanishes. Across the different metamaterials, the Casimir-Polder interaction is characterized by the usual real coefficient leading to a dispersive resonance and also by a dissipative response. Here, the atomic excitation is resonantly transmitted to a surface plasmon, and eventually lost in the metamaterial. A simple model, considering only the resonant exchange of photons between atoms and the metamaterial in the mean-field approximation, is able to reproduce the shape of the Casimir-Polder resonance but predicts a smaller contribution. This comparison suggests that enhancement of the Casimir-Polder interaction inherent to the metamaterial should be present.

The work was supported by the Singapore Ministry of Education Academic Research Fund Tier 3 (Grant No. MOE2011-T3-1-005). A.L. thanks the UMI Majulab and the Centre for Quantum Technologies for supporting his trip to Singapore.

* martial.ducloy@univ-paris13.fr
† david.wilkowski@ntu.edu.sg

[1] J. E. Lennard-Jones, Transactions of the Faraday Society **28**, 333 (1932), ISSN 0014-7672.
[2] F. London, Transactions of the Faraday Society **33**, 8b (1937), ISSN 0014-7672.
[3] H. B. G. Casimir and D. Polder, Physical Review **73**, 360 (1948).
[4] E. M. Lifshitz, Sov. Phys. JETP **2**, 73 (1956).
[5] I. E. Dzyaloshinskii, E. M. Lifshitz, and L. P. Pitaevskii, Soviet Physics Uspekhi **4**, 153 (1961), ISSN 0038-5670.
[6] A. McLachlan, Molecular Physics **7**, 381 (1964), ISSN 0026-8976, 1362-3028.
[7] D. Raskin and P. Kusch, Physical Review **179**, 712 (1969), ISSN 0031-899X.
A. Shih, D. Raskin, and P. Kusch, Physical Review A **9**, 652 (1974), ISSN 0556-2791.
A. Anderson, S. Haroche, E. A. Hinds, W. Jhe, and D. Meschede, Physical Review A **37**, 3594 (1988), ISSN 0556-2791.
[8] J. Woerdman and M. Schuurmans, Optics Communications **14**, 248 (1975), ISSN 0030-4018.
A. Akulshin, V. Velichanskii, A. Zibrov, V. Nikitin, V. Sautenkov, E. Yurkin, and N. Senkov, Jetp Letters **36**, 303 (1982), ISSN 0021-3640, wOS:A1982QP81200007.
M. Oria, M. Chevrollier, D. Bloch, M. Fichet, and M. Ducloy, EPL (Europhysics Letters) **14**, 527 (1991), ISSN 0295-5075.
[9] M. Chevrollier, M. Fichet, M. Oria, G. Rahmat, D. Bloch, and M. Ducloy, Journal de Physique II **2**, 631 (1992), ISSN 1155-4312, 1286-4870.
[10] M. Fichet, G. Dutier, A. Yarovitsky, P. Todorov, I. Hamdi, I. Maurin, S. Saltiel, D. Sarkisyan, M.-P. Gorza, D. Bloch, et al., Europhysics Letters (EPL) **77**, 54001 (2007), ISSN 0295-5075, 1286-4854.
[11] A. Landragin, J.-Y. Courtois, G. Labeyrie, N. Vansteenkiste, C. I. Westbrook, and A. Aspect, Physical Review Letters **77**, 1464 (1996), ISSN 0031-9007, 1079-7114.
[12] J. M. Obrecht, R.J. Wild, M. Antezza, L.P. Pitaevskii, S. Stringari, and E. A. Cornell, Physical review letters **98**, 063201 (2007).
[13] J. Reichel and V. Vuletic, eds., Atom chips (Wiley-VCH, Weinheim, Germany, 2011), ISBN 978-3-527-40755-2, oCLC: ocn664325852.
[14] M. Gullans, T. G. Tiecke, D. E. Chang, J. Feist, J. D. Thompson, J. I. Cirac, P. Zoller, and M. D. Lukin, Physical Review Letters **109**, 235309 (2012).
[15] D. Chang, K. Sinha, J. Taylor, and H. Kimble, Nature communications **5** (2014).
[16] H. Failache, S. Saltiel, M. Fichet, D. Bloch, and M. Ducloy, Physical Review Letters **83**, 5467 (1999), ISSN 0031-9007, 1079-7114.
H. Failache, S. Saltiel, M. Fichet, D. Bloch, and M. Ducloy, The European Physical Journal D - Atomic, Molecular, Optical and Plasma Physics **23**, 237 (2003), ISSN 1434-6060, 1434-6079.
[17] M.-P. Gorza, S. Saltiel, H. Failache, and M. Ducloy, The European Physical Journal D **15**, 113 (2001), ISSN 14346060.
[18] A. Laliotis, T. P. de Silans, I. Maurin, M. Ducloy, and D. Bloch, Nature Communications **5** (2014), ISSN 2041-1723.
[19] H. Failache, S. Saltiel, A. Fischer, D. Bloch, and M. Ducloy, Physical Review Letters **88**, 243603 (2002).
[20] S. A. Aljunid, E. A. Chan, G. Adamo, M. Ducloy, D. Wilkowski, and N. I. Zheludev, Nano Letters **16**, 3137 (2016), ISSN 1530-6984.
[21] J. Baker-Jarvis, E. Vanzura, and W. Kissick, IEEE Transactions on Microwave Theory and Techniques **38**, 1096 (1990), ISSN 0018-9480.
X. Chen, T. M. Grzegorczyk, B.-I. Wu, J. Pacheco, and J. A. Kong, Physical Review E **70**, 016608 (2004).
J. Qi, H. Kettunen, H. Wallen, and A. Sihvola, in 2010 URSI International Symposium on Electromagnetic Theory (EI (2010), pp. 588–591.
X.-X. Liu and A. Alu, Physical Review B **87**, 235136 (2013).
[22] M. Ducloy and M. Fichet, Journal de Physique II **1**, 1429 (1991), ISSN 1155-4312, 1286-4870.
[23] M. Chevrollier, M. Oriá, J. G. de Souza, D. Bloch, M. Fichet, and M. Ducloy, Physical Review E **63**, 046610 (2001).
[24] J. M. Wylie and J. E. Sipe, Physical Review A **30**, 1185 (1984), ISSN 0556-2791.
[25] M. Fichet, F. Schuller, D. Bloch, and M. Ducloy, Physical Review A **51**, 1553 (1995), ISSN 1050-2947, 1094-1622.
[26] A. Laliotis and et *al.* (unpublished).